Research Article

Shake Table Study on the Efficiency of Seismic Base Isolation Using Natural Stone Pebbles

Ivan Banović [ID]**, Jure Radnić, and Nikola Grgić** [ID]

University of Split, Faculty of Civil Engineering, Architecture and Geodesy, Matice Hrvatske 15, 21000 Split, Croatia

Correspondence should be addressed to Ivan Banović; ivan.banovic@gradst.hr

The results of a shake table study of the efficiency of a seismic base isolation using a layer of natural stone pebbles are presented. Models of stiff and medium-stiff buildings were tested. Case studies were conducted with the foundation of model on the rigid base and on four different layers of pebbles (thin and thick layer with small and large pebbles). Four different horizontal accelerograms were applied, and the characteristic displacements, accelerations, and strains were measured. Strains/stresses of the tested models remained in the elastic area. It was concluded that the effectiveness of the stone pebble layer under the foundation, i.e., the reduction in the seismic forces and stresses in the structure compared to the classical solution of foundation, significantly depends on the type of the applied excitation and depends relatively little on the layer thickness and pebble fraction. The results of the study showed that a layer of pebbles can significantly reduce the peak acceleration and strains/stresses of the model, with acceptable displacements. Further research is expected to confirm the effectiveness of this low-cost and low-tech seismic base isolation and to pave the way to its practical application.

1. Introduction

Modern science in recent decades has explored numerous solutions to reduce the seismic forces on buildings, aiming to improve safety during earthquakes and to provide more rational solutions. Some of these aseismic solutions are quite simple and rational (e.g., different variants of elastomeric bearings) and have found applications in the construction of bridges and important buildings. Unfortunately, a large number of the devices for reducing the seismic forces on structures and for controlling their displacements in the earthquake remain complex and expensive, and their practical application remains rare. To enable widespread application of a solution for seismic isolation, especially in less-developed countries, it should be simple and based on low technology.

Solutions involving the application of a layer of appropriate materials under the foundation to reduce seismic forces on buildings, which are expected to be efficient and rational for use in the so-called low-cost buildings, are the starting point of our study. Such a low-cost and low-technology method could be widely used in seismic isolation of low-rise buildings around the world. The research

results of one such seismic isolation method are presented in this paper.

There are indications that in ancient history, builders used layers of different materials to increase the seismic resistance of buildings. Contemporary researchers are exploring this ancient approach to find the appropriate solutions that enable replacement of sophisticated devices for seismic isolation in many buildings with simple methods. Currently, to the author's knowledge, there are very few studies related to the use of natural materials for seismic base isolation of buildings.

A concept of interposing an artificial soil layer between the superstructure and the foundation soil was examined by Doudoumis et al. [1]. Extended investigation of utilization of a smooth synthetic liner placed within the soil deposit can be found in [2, 3]. Xiao et al. [4] tested five potential isolation materials to characterize their frictional features by both semidynamic and shake table experiments. The materials were sand, lighting ridge pebble, polypropylene sheet, PVC sheet, and polythene membrane. A series of numerical simulations and a parametric study on seismic base isolation using rubber-soil mixtures can be found in [5]. Radnić et al.

[6, 7] found from shake table tests that a thin layer of plain sand under the foundation can reduce seismic forces to a cantilever concrete column by over 10%. Xiong and Li [8] analyzed seismic base isolation using rubber-soil mixtures (RMSs) based on shake table tests and a parametric numerical study in [9]. The effectiveness of utilizing a rubber-sand mixture (RSM) in the foundation soil of different moment-resisting frame (MRF) typologies was assessed through numerical simulations in [10]. The results highlighted the beneficial effects of the use of RSM as a foundation layer on the structures' response under dynamic loading, particularly for the mid- and high-rise buildings, leading to a reduction in the base shear and maximum interstory drift up to 40% and 30%, respectively, in comparison with the clean sand profile. Panjamani et al. [11] obtained similar results in terms of acceleration and interstory drift reduction; at different floor levels with the use of RSM, the reduction can be approximately 40 to 50%. Bandyopadhyay et al. [12] found from shake table tests that a composite consisting of sand and 50% shredded rubber tire placed under the foundation was most promising as a low-cost effective base isolator. Patil et al. [13] found encouraging results regarding the efficiency of seismic base isolation using river sand based on experimental and analytical work. Nanda et al. [14–17] conducted experimental studies based on shake table tests by providing geotextiles and a smooth marble frictional base isolation system at the plinth level of a brick masonry building. A 65% reduction in absolute response acceleration at the roof level was obtained in comparison with the response of the fixed base structure. Further work on pure-friction base isolation systems can be found in [18, 19].

This paper presents the results of a shake table study regarding the efficiency of seismic base isolation using natural stone pebbles below the foundation for the reduction in seismic forces on structures, with the aim that such a solution finds practical application in the construction of low-cost buildings and smaller bridges in seismically active regions. Testing was performed on stiff and medium-stiff buildings. Four different accelerograms were applied, and stresses of the models remained in the elastic area. First, a model with the foundation directly on a rigid base (shake table) was tested, and then a model with a layer of stone pebbles under the foundation (the layer thickness and fraction of the pebbles are varied) was tested. Characteristic displacements, accelerations, and strains were measured. Some study results are presented and discussed, and the main conclusions of the research are given at the end of the paper. However, further research on some important effects that were not considered in this study is required to achieve even more reliable conclusions regarding the efficiency and rationality of the considered concept of seismic isolation.

2. Layer of Natural Stone Pebbles below the Foundation

Stone pebbles are natural material created from larger pieces of stone under the long-lasting action of rivers and sea. In this process, the sharp parts of stone were rounded, and the weak parts of stone have fallen off as a result only solid, smooth, rounded pieces of stone (stone pebbles) remain. In this study, stone pebbles from a riverbed were used. The pebbles are mainly of limestone and partly of granite. In the conducted tests, the following two fractions of pebbles were used (Figure 1): 4–8 mm (i.e., small pebbles) and 16–32 mm (i.e., large pebbles). The average compressive strength of the pebbles was approximately 80 MPa, and the humidity was approximately 10%. It is assumed that the thickness of the pebble layer of approximately 0.3 to 1.0 m could be effective in terms of reducing the seismic forces to the building, while being a rational approach. A thicker layer is probably more efficient but requires deeper excavation and a taller embankment, i.e., higher costs. In the conducted tests, the following two layer thicknesses were used (Figure 2): $d = 0.3$ m (thin layer) and $d = 0.6$ m (thick layer). Layers are formed within a frame with a plan size of 2.5 m × 2.5 m, which was fixed to the shake table. The deformation conditions of the layer within the frame are sought to be similar to those that the layer would have under the foundation of a real building. Although a reduced model of the building was used, the layer thickness was used in real size because the reduced building model has the same dynamic characteristics (periods of free oscillations) as that of the target full-scale building. The layers were formed in sub-layers with a thickness of 0.10 m, with static compaction and dynamic compaction using the shake table. The average compaction module at the top of the layer was approximately MS = 30 MPa.

3. Adopted Building Models

Seismic forces on the structure significantly depend on their dynamic characteristics, i.e., on the structure stiffness and the weight. The dynamic characteristics of the building are well described by its periods and forms of free oscillations. According to [20], for type 1 and type of ground soil A, spectral acceleration S_e for a elastic single-degree-of-freedom (SDOF) system of a cantilever column with mass on its top is defined according to the fundamental free oscillation period T (Figure 3). Real buildings have a wide stiffness range, from very stiff to very soft, i.e., a wide spectrum of T.

Instead of a small-scale model of a real building, which results in a series of problems and doubts, a model (cantilever column with a mass on top—SDOF) that has the same fundamental period T as a real building is adopted in this study. Thus, this model well represents the dynamic characteristics of the real building. Two models of buildings shown in Figure 4 were tested: the MSB model with $T = 0.05$ s which represents stiff buildings and the MSSB model with $T = 0.6$ s which represents medium-stiff buildings (Figure 3). The adopted models include a foundation because the behavior of real buildings in the earthquake depends significantly on their foundations, i.e., on the soil-structure interaction. The calculation of the seismic forces based on an SDOF system starts from the assumption that there is no displacements and rotations of the column bottom, i.e., there is no displacement and rotation of the foundation. This study takes these effects into consideration.
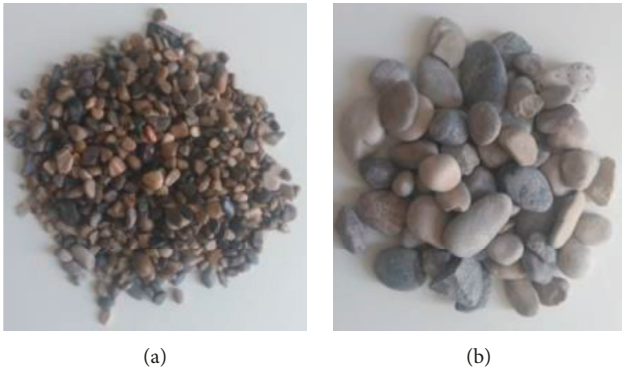
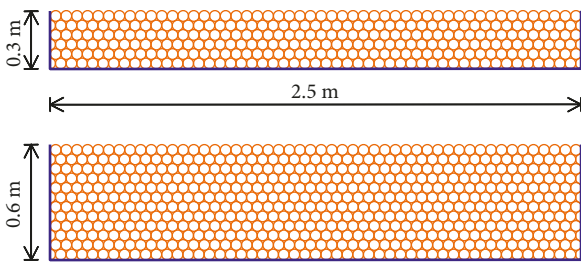Figure 1: Used fractions of pebbles. (a) 4–8 mm. (b) 16–32 mm.
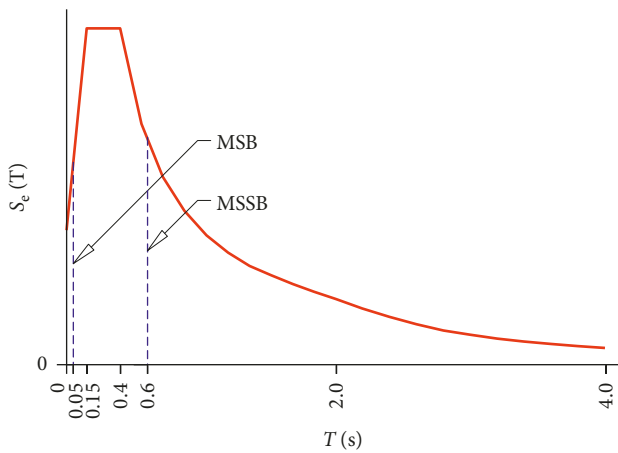

Figure 2: Used thicknesses of pebble layer.

Figure 3: Seismic response spectra according to [20], for type 1 and type of ground soil A.

Figure 4: Considered building models. (a) MSB ($T = 0.05$ s). (b) MSSB ($T = 0.60$ s).

The same foundation and mass on the top of the column were adopted in both models, with different column heights and dimensions of its cross section. The foundation and mass at the top of the column ($m = 1000$ kg) are made from concrete (cube strength of 46 MPa), and the column is a square steel tube with uniaxial tensile strength of 355 MPa. The foundation is highly reinforced and is practically rigid. In the conducted experimental tests, relatively small plan dimensions of the foundation were adopted. However, they are the same in the case of the foundation supported on the rigid base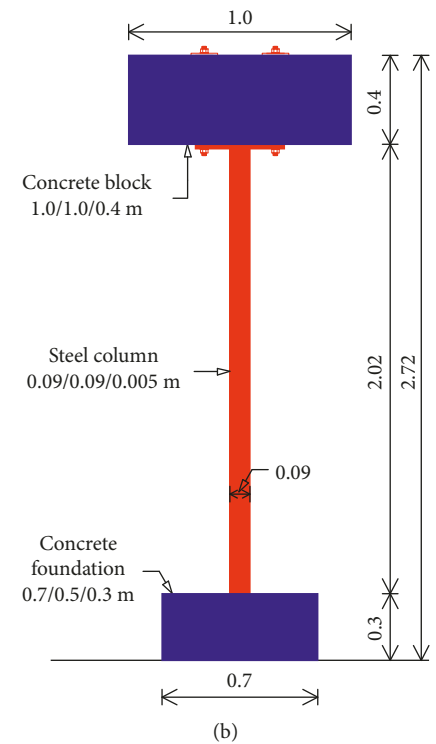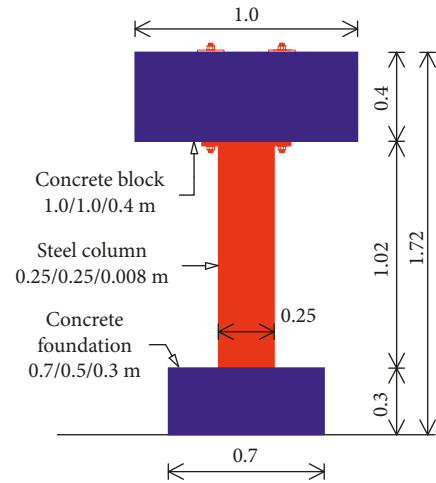 and on the pebble layers. In further research, it is planned to vary the different plan dimensions of the foundation. In the adopted steel columns, stresses remained in the elastic area for all performed tests. Namely, the starting point was that for all tests, nonlinearity does not appear in the whole structure (column and foundation), i.e., all nonlinearity and dissipation of seismic energy are realized in the pebble layer and in the layer-foundation coupling surface. Thus, the intention was to exclude the influence of nonlinearity in the construction material, i.e., the dissipation of seismic energy in the form of plastification and damage of the construction material, on the results regarding the aseismic efficiency of the tested pebble layer.

4. Tested Samples

Ten different samples were experimentally tested (Figure 5) under four different types of dynamic excitation produced by the shake table. The first tested MSB and MSSB models were supported on a rigid base P_r (Figure 5(a)). A concrete layer was placed and fixed on the top of the shake table to simulate the usual subconcrete under foundation of a real building. This situation approximates the real buildings with a classic foundation without seismic base isolation. The horizontal displacement of the foundation in relation to the base (shake table) is prevented, while the rocking and uplifting of the foundation is allowed. Next, MSB and MSSB models supported on different layers of pebble (P_{p1} to P_{p4}) were tested (Figure 5(b)). The layer thickness d (0.3 m and 0.6 m) and the pebble fraction Φ (4 to 8 mm and 16 to 32 mm) were varied. The pebble layer was returned to its initial condition after each test, i.e., recompaction to the required compaction module and leveling of the layer top. The same shake table acceleration was adopted for the model supported on a rigid base and on a pebble layer. It is assumed that the real earthquake acceleration at the top of the natural solid ground in both cases is the same.

5. Dynamic Excitations

The models of buildings with considered variants of foundation support (Figure 5) were exposed to horizontal accelerations of the shake table in the direction of larger dimension of the foundation, using the accelerograms shown in Figure 6. The maximum acceleration $a_{g,max}$ of the accelerogram is scaled to 0.3 g and 0.2 g for the MSB and MSSB model, respectively. An artificial accelerogram (AA), as shown in Figure 6(a), is created to match the elastic response spectra according to [20]. The horizontal component N-S of the Petrovac earthquake (Montenegro) [21] is shown in Figure 6(b) (AP), the horizontal component N-S of the Ston earthquake (Croatia) [21] is shown in Figure 6(c) (AS), and the horizontal component N-S of the Banja Luka earthquake (BiH) [21] is shown in Figure 6(d) (ABL). Elastic response spectra of the adopted accelerograms are shown in Figure 7. It is difficult to predict which applied accelerogram will be most unfavorable for each tested sample in Figure 5 because of the possible occurrence of nonlinearities in the system. The adopted accelerograms cover a wide spectrum of potential earthquake types. Namely, the artificial accelerogram (AA) is characterized by the long-lasting action, moderate predominant period, large spectral displacements, and high earthquake input energy in structure. Compared to AA, accelerogram Petrovac (AP) has similar characteristics, slightly shorter duration and longer predominant period. The Ston accelerogram (AS) and B. Luka accelerogram (ABL) are characterized by a short impact action with a short predominant period. Namely, AS and ABL represent the so-called impact earthquakes.

6. Measured Values

The following values were measured on each tested sample (Figure 8): horizontal displacement of the mass center at the column top (u_1), horizontal displacement at the foundation top (u_2), vertical displacement at the right edge (v_1) and at the left edge (v_2) of the foundation, vertical strain on the bottom of the steel column at the right side (ε_1) and at the left side (ε_2), and horizontal acceleration of the mass center at the column top (a).

7. Testing and Measuring Equipment

Tests were performed using a shake table at the University of Split, Faculty of Civil Engineering, Architecture and Geodesy (Croatia). Data collection from all sensors was performed using the Quantum-x mx 840A system (HBM). The displacements were measured using analog displacement sensors, type PB-25-S10-N0S-10C (Uni Measure). The strains were measured using strain gauges, type 6/120 LY11 (HBM). The accelerations were measured by a piezo-electric low frequency accelerometer type 4610 (MS). Some photos of experimental setup before testing are shown in Figure 9.

8. Experimental Results

The test results are shown in a graphic form to ensure that the presentation is concise and clear, even with reduced size of the drawings. The results are separately shown for some of the measured values, for the models MSB and MSSB. Each of the drawings shows the measured values separately at each applied accelerogram, for all five considered substrate types: P_r—rigid base; P_{p1}—pebble layer ($d = 0.3$ m, $\Phi = 16$ to 32 mm); P_{p2}—pebble layer ($d = 0.6$ m, $\Phi = 16$ to 32 mm); P_{p3}—pebble layer ($d = 0.3$ m, $\Phi = 4$ to 8 mm); and P_{p4}—pebble layer ($d = 0.6$ m, $\Phi = 4$ to 8 mm); see Figure 5.

In order to investigate the impact of some possible negative factors on the conclusions of the study, preliminary research has been carried out. Namely, in order to investigate the impact of subsequent earthquakes on the efficiency of the considered seismic base isolation, the tested structure was exposed to a set of six repeated base accelerations, without updating the pebble layer. Testing was performed with AA and AS, for MSB on layer P_{p1} (Figure 5) and MSSB on layer P_{p4}. Compared to the first excitation, repeated excitations produced up to 8.6% higher strain/stress on the bottom of the steel column and up to 196% larger irreversible horizontal displacement at the foundation top. This can be considered acceptable because it is unlikely that some buildings would be exposed to a large number of medium to severe earthquakes that would cause building displacements in the same direction. To prevent a possible similar scenario, the problem can be solved so that the width of the aseismic layer is sufficiently wider than the foundation.

Tests with repeated high base accelerations that could cause nonlinearities in the model were not performed. The pebble layer efficiency for repeated base accelerations is explained by the fact that the layer of stone pebbles of the same grain size is very difficult to compact. Also, the influence of compaction of P_{p1} and P_{p4} layers was also tested with AA and AS. The average compaction module at the top of the layers was MS = 30 MPa and MS = 60 MPa, respectively. The maximum strain/stress on the bottom of the
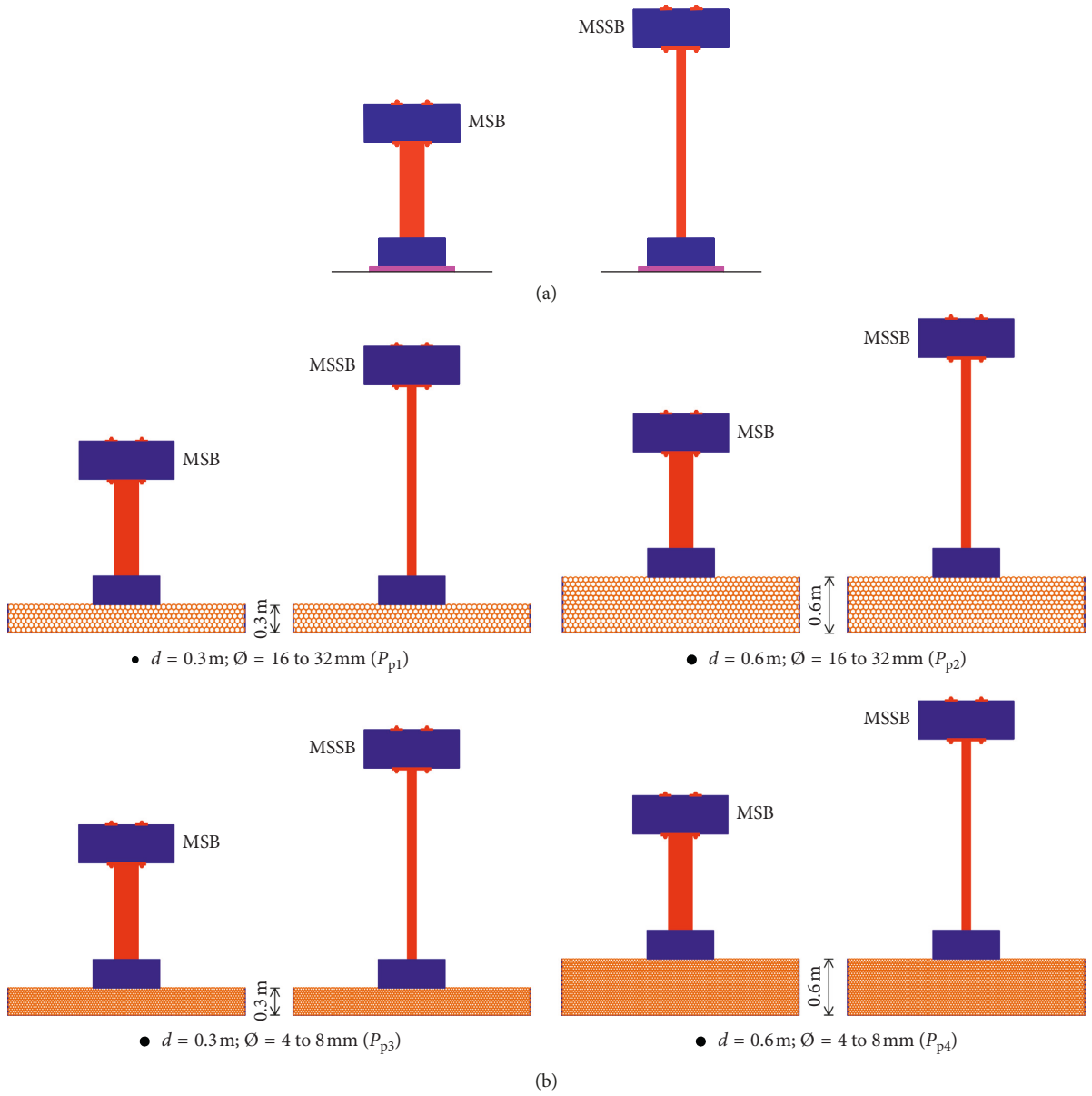
(a)

MSB

MSSB

MSB

MSSB

0.3 m

● $d = 0.3$ m; Ø = 16 to 32 mm (P_{p1})

MSB

MSSB

0.6 m

● $d = 0.6$ m; Ø = 16 to 32 mm (P_{p2})

MSB

MSSB

0.3 m

● $d = 0.3$ m; Ø = 4 to 8 mm (P_{p3})

MSB

MSSB

0.6 m

● $d = 0.6$ m; Ø = 4 to 8 mm (P_{p4})

(b)

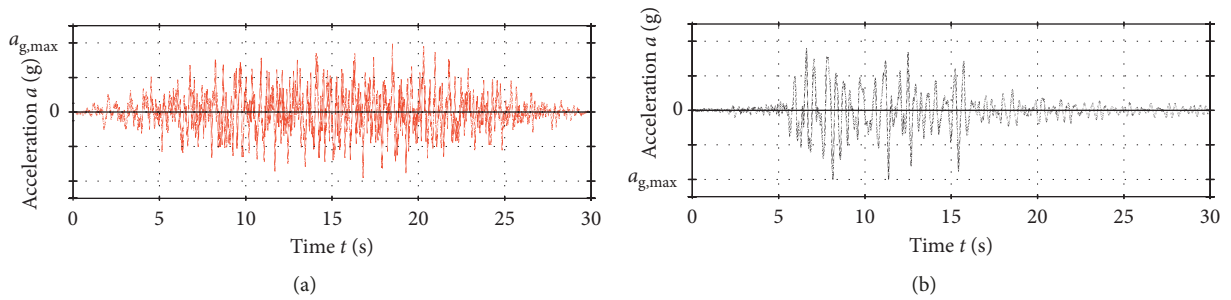FIGURE 5: Tested samples. (a) Rigid base (P_r). (b) Pebble layers.

(a)

(b)

FIGURE 6: Continued.

(c)

(d)
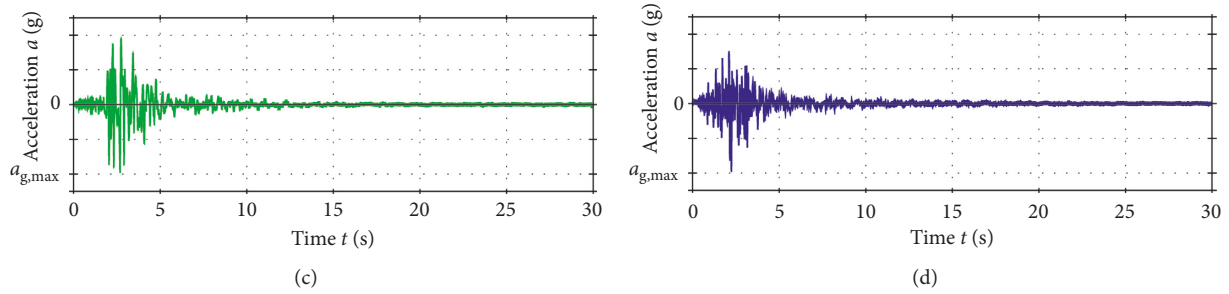
FIGURE 6: Applied horizontal base accelerations ($a_{g,max}$ scaled to 0.2 g for MSSB and 0.3 g for MSB). (a) Artificial accelerogram (AA). (b) N-S accelerogram of Petrovac earthquake (AP). (c) N-S accelerogram of Ston earthquake (AS). (d) N-S accelerogram of B. Luka earthquake (ABL).
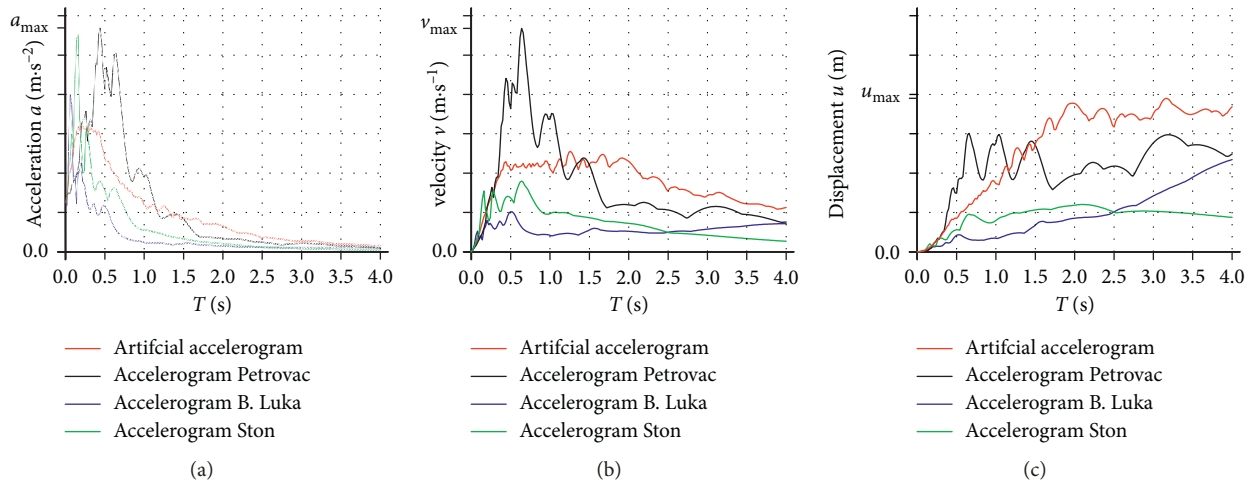

(a)

(b)

(c)

FIGURE 7: Elastic response spectra for applied accelerograms. (a) Spectral acceleration. (b) Spectral velocity. (c) Spectral displacement.
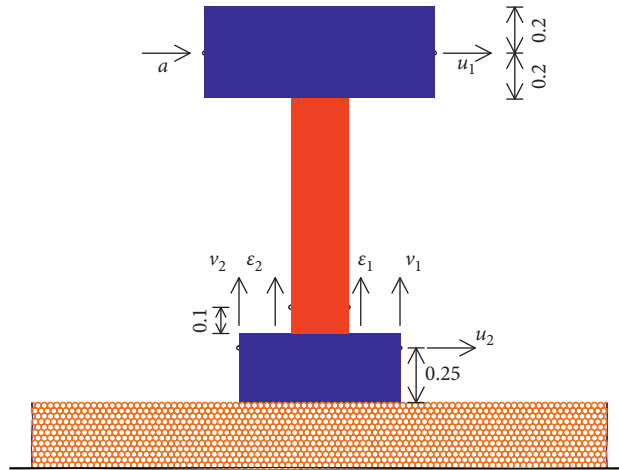

FIGURE 8: Measured values.

steel column for MS = 60 MPa was 4.9% higher than for MS = 30 MPa. This can be considered acceptable.

Foregoing suggests that the proposed seismic base isolation can be effective throughout the lifetime of the building and it is not necessary to renew.

8.1. Model of Stiff Building MSB. Horizontal acceleration of the mass center at the column top (a) is shown in

Figure 10. It is found that the rigid base produced maximum acceleration for all considered accelerograms and that the maximum accelerations for the pebble layer were similar. Compared to the rigid base, thin layer with large pebbles produced the lowest reduction in acceleration. For $a_{g,max} = 3.0$ m·s^{-2}, the highest acceleration on the rigid base was produced by AA (approx. 11.6 m·s^{-2}), whereas the lowest was produced by ABL (approx. 5.8 m·s^{-2}). The maximum acceleration with a pebble layer
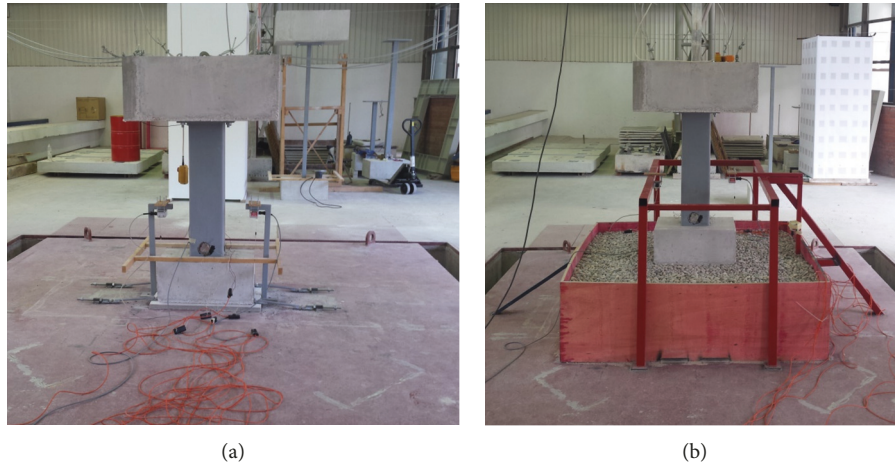
(a)

(b)

FIGURE 9: Photos of experimental setup before testing. (a) MSB on rigid base. (b) MSB on layer P_{p2}.
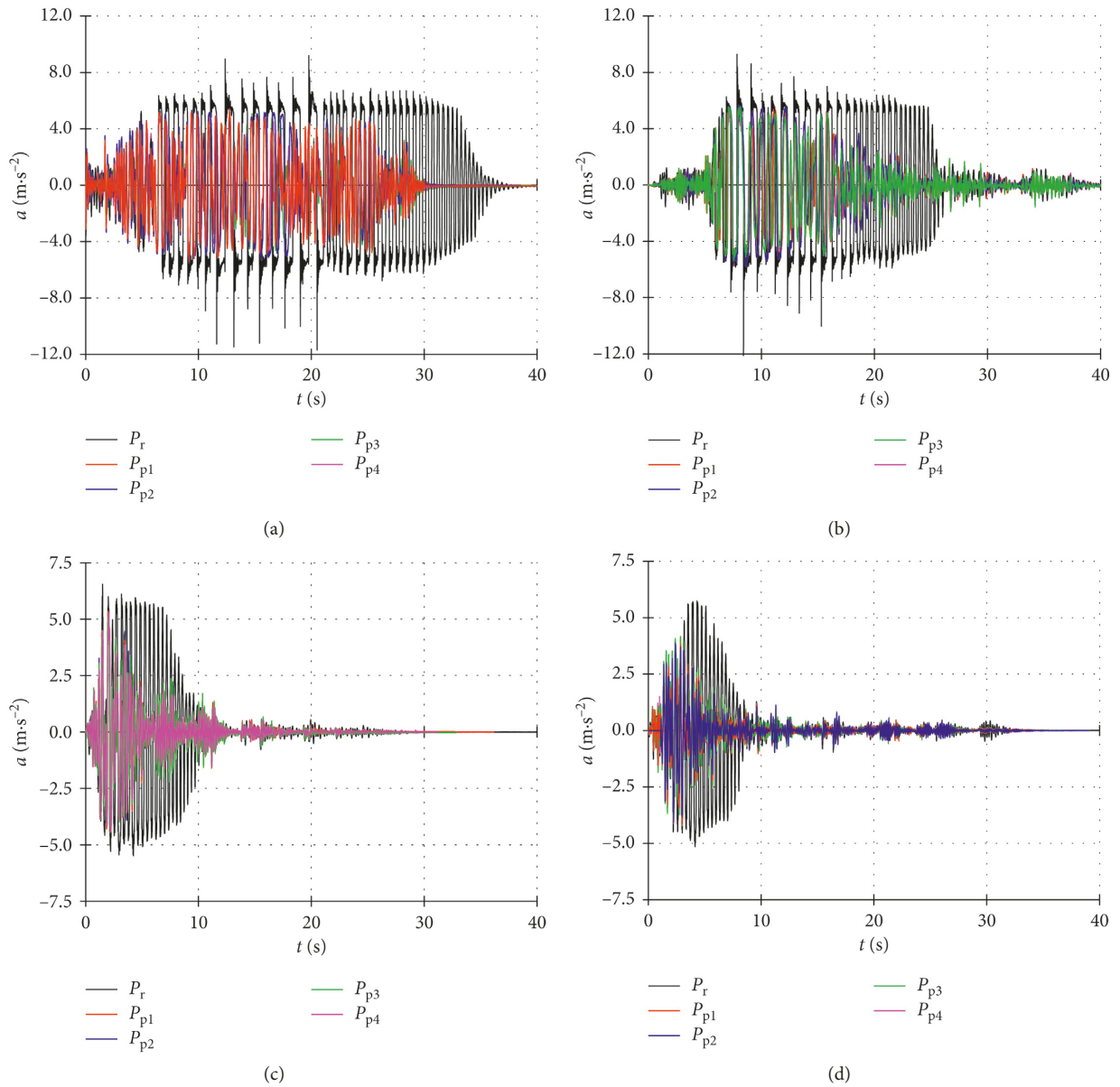

(a)

(b)

(c)

(d)

FIGURE 10: Horizontal acceleration of the mass center at the column top (a) for MSB. (a) Artificial accelerogram (AA). (b) Accelerogram Petrovac (AP). (c) Accelerogram Ston (AS). (d) Accelerogram B. Luka (ABL).
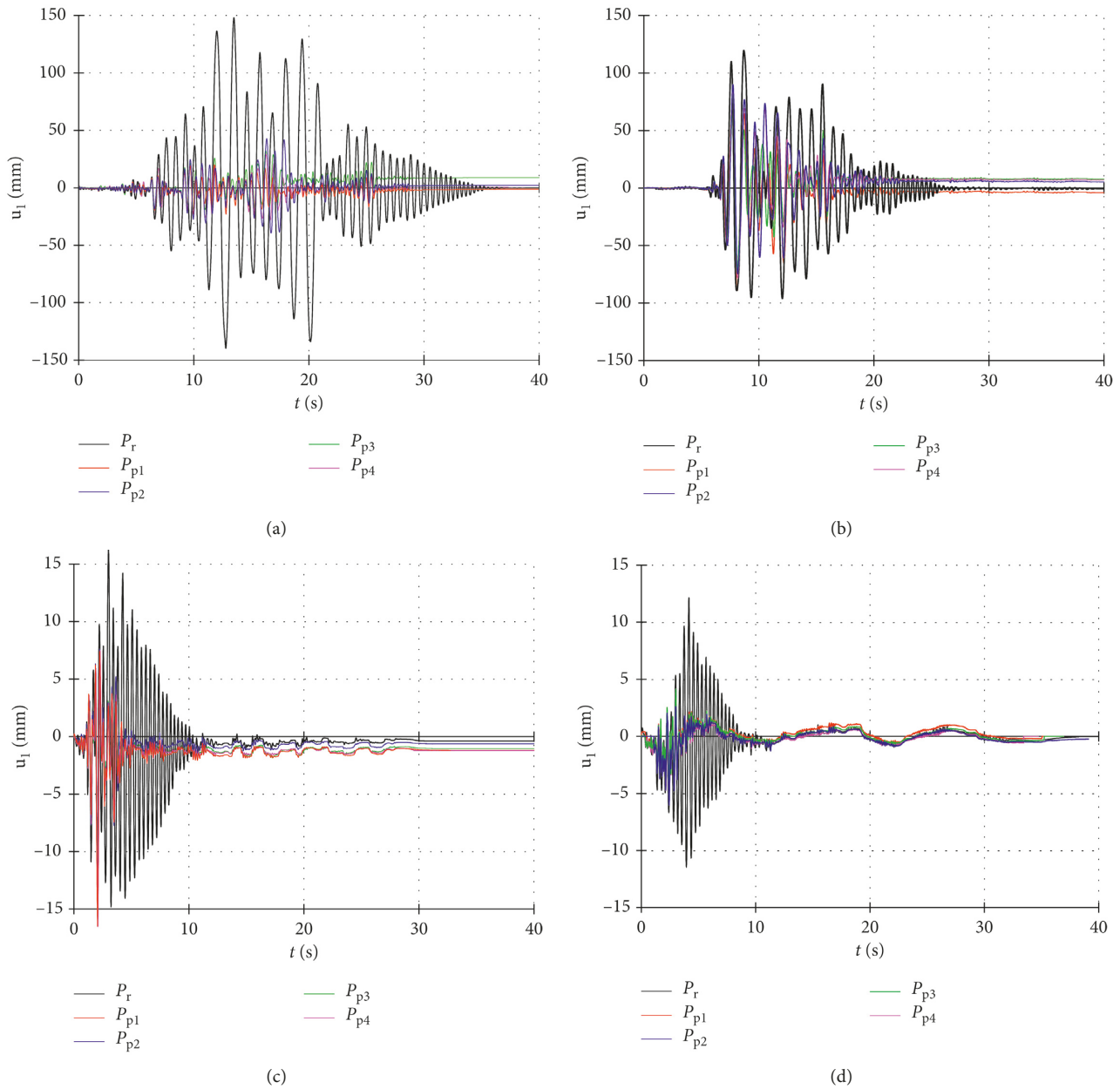
FIGURE 11: Horizontal displacement of the mass center at the column top (u_1). (a) Artificial accelerogram (AA). (b) Accelerogram Petrovac (AP). (c) Accelerogram Ston (AS). (d) Accelerogram B. Luka (ABL).

for AA and ABL was approx. $5.7\,\mathrm{m\cdot s^{-2}}$ and approx. $4.1\,\mathrm{m\cdot s^{-2}}$, respectively.

The largest horizontal displacement of the mass center at the column top (u_1) for all considered accelerograms was produced with the rigid base, and the maximum displacements on all pebble layers were similar (Figure 11). Compared to the rigid base, the slightest reduction in the displacement was produced using a thin layer with large pebbles. For the rigid base, AA produced the largest displacement of approximately 150 mm, whereas ABL produced the smallest displacement of approximately 12 mm. The largest displacement on the pebble layer was produced by AP (approx. 80 mm), whereas the smallest was produced by ABL (approx. 3.5 mm).

The vertical strain on the right bottom side of the steel column (ε_1) is presented in Figure 12. Note that the model on the rigid base had the maximum strain for all considered accelerograms and that the maximum strain for the model on the pebble layers was similar. Compared to the rigid base, the slightest reduction in strain also produced a thin layer with large pebbles. The largest strain on the rigid base was caused by AP (approx. 0.059‰), whereas the smallest was caused by ABL (approx. 0.018‰). The largest strain on the pebble layer was caused by AP (approx. 0.028‰), whereas the smallest was caused by ABL (approx. 0.018‰). All strains (stresses) were within the elastic area of the steel ($\leq 1.7‰$).
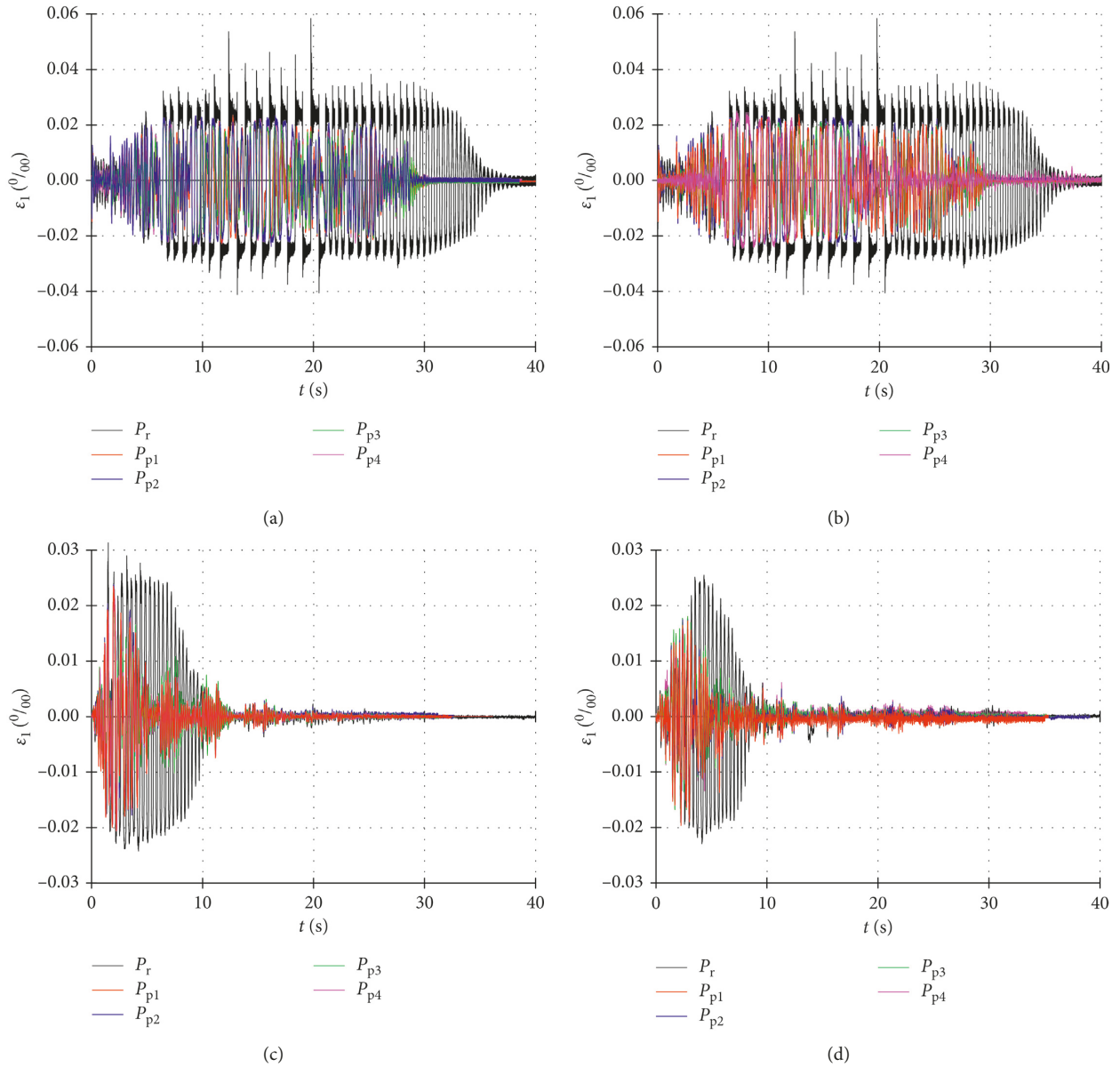
FIGURE 12: Vertical strain on the right bottom side of the steel column (ε_1) for MSB. (a) Artificial accelerogram (AA). (b) Accelerogram Petrovac (AP). (c) Accelerogram Ston (AS). (d) Accelerogram B. Luka (ABL).

The horizontal displacement at the foundation top (u_2) is prevented for a rigid base (Figure 13), i.e., the bottom of the foundation is fixed to the base (shake table). The largest displacement for the pebble layer was produced by AP (approx. 18.5 mm), whereas the smallest was produced by ABL (approx. 1.2 mm). Thicker layers resulted in larger horizontal displacements. The largest permanent displacement for the pebble layer was produced also by AP (approx. 6.0 mm), which is the result of the foundation slipping at the pebble layer top. Thus, the ratio of the largest permanent displacement of the foundation and peak foundation displacement for AP is approximately 6 mm : 18.5 mm or about 1 : 3.

The largest uplifts of the foundation (Figure 14) were produced for models with the rigid base, approximately 64 mm for AA and approximately 4.4 mm for ABL. The largest uplift of the foundation for the pebble layer was produced by AP (approx. 35 mm), whereas the smallest was produced by ABL (approx. 1.8 mm). The largest permanent settlement on the left edge of the foundation of approximately 7 mm was produced by AP (thin layer with large pebbles).

8.2. Model of Medium-Stiff Building MSSB.

Horizontal acceleration of the mass center at the column top (a) is shown in Figure 15. It can be seen that the rigid base produced maximum acceleration for all applied accelerograms and that the maximum accelerations for the pebble layer were similar (analogous to model MSB). For $a_{g,max} = 2.0 \, \text{m·s}^{-2}$, the
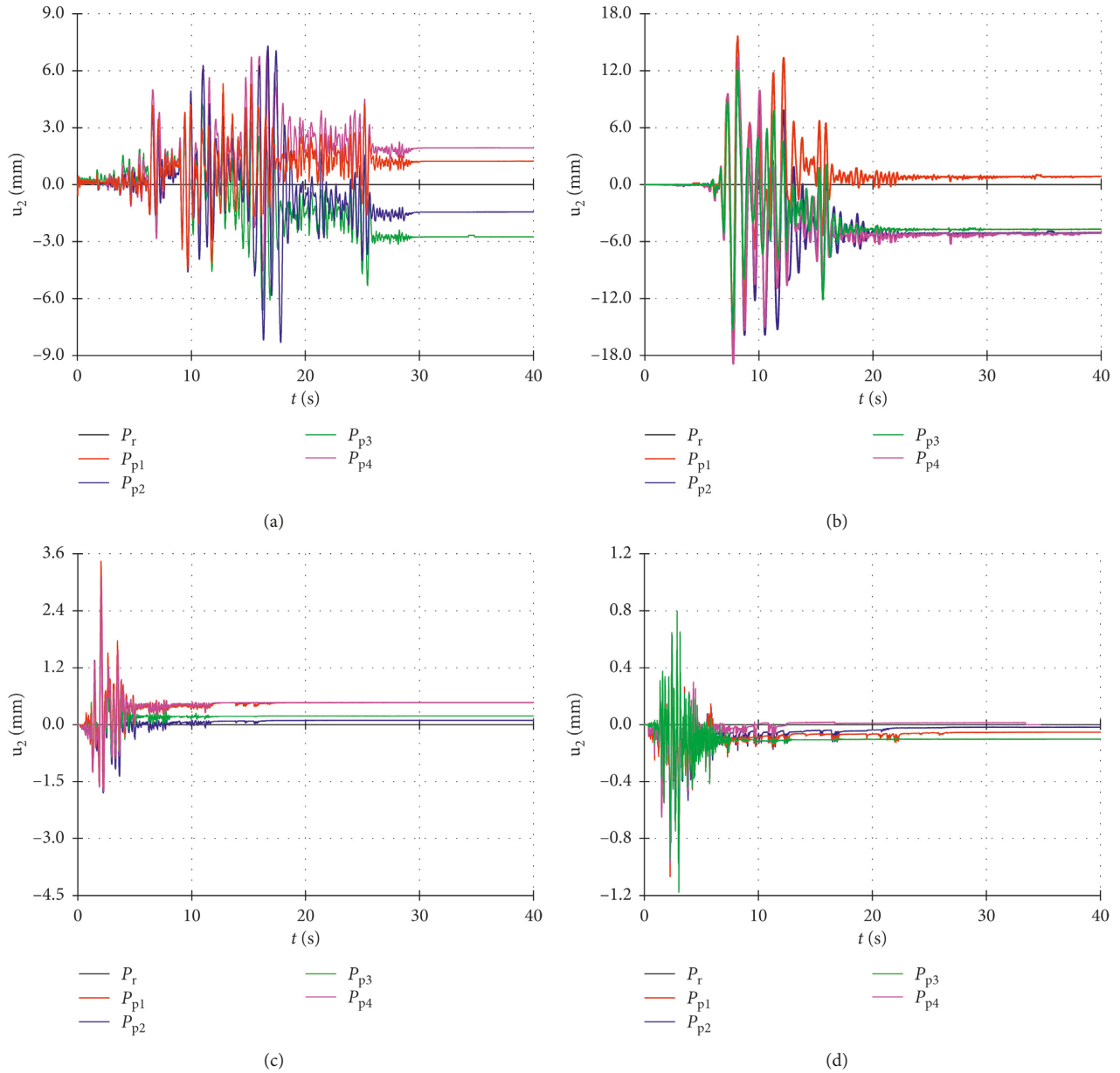
(a)

(b)

(c)

(d)

FIGURE 13: Horizontal displacement at the foundation top (u_2) for MSB. (a) Artificial accelerogram (AA). (b) Accelerogram Petrovac (AP). (c) Accelerogram Ston (AS). (d) Accelerogram B. Luka (ABL).

highest acceleration for the model on the rigid base was produced by AA and AP (approx. 7.5 m·s^{-2}), whereas the lowest was produced by ABL (approx. 2.8 m·s^{-2}). The maximum acceleration with a pebble layer for AA and ABL was approximately 4.4 m·s^{-2} and approximately 2.4 m·s^{-2}, respectively.

The largest horizontal displacements of the mass center at the column top (u_1) were also for the rigid base case (Figure 16): AA produced the largest displacement of approximately 170 mm, whereas ABL produced the smallest of approximately 21.5 mm. The largest displacement for the model on the pebble layer was produced by AP (approx. 110 mm), whereas the smallest was produced by ABL (approx. 21.5 mm). The largest permanent displacement

on the pebble layer was for AA (approx. 25 mm), which is the result of the foundation slipping at the pebble layer top and foundation rotation on the vertically deformable substrate.

The vertical strain on the right bottom side of the steel column (ε_1) is presented in Figure 17. The maximum strain for the rigid base was approximately equal for AA and AP (approx. 0.82‰), i.e., within the elastic steel behavior. The minimum strain was for ABL (approx. 0.33‰). Compared to the MSB model, the MSSB model had significantly greater stresses/strains. For the pebble layer, AA produced maximum strain of approximately 0.45‰.

The largest displacement at the foundation top (u_2) for the pebble layer (Figure 18) was produced by AA (approx.
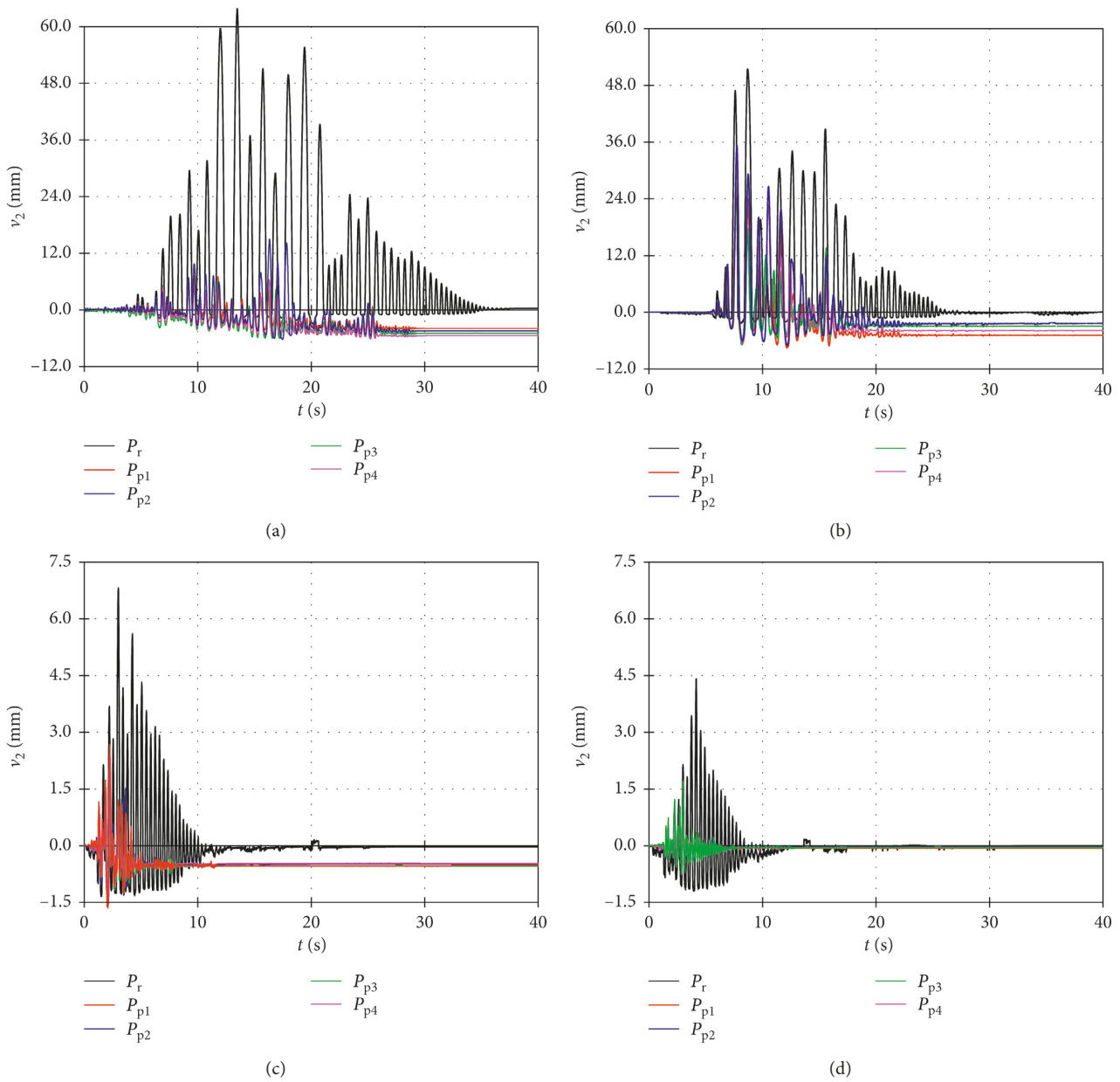
FIGURE 14: Vertical displacement at the left edge of the foundation (v_2) for MSB. (a) Artificial accelerogram (AA). (b) Accelerogram Petrovac (AP). (c) Accelerogram Ston (AS). (d) Accelerogram B. Luka (ABL).

13 mm), whereas the smallest was produced by ABL (approx. 1.6 mm). The largest permanent displacement (u_2) for the pebble layer was for AA (approx. 7 mm) with a thick layer of large pebbles, as a result of the foundation sliding on the pebble layer top.

The largest uplift at the left edge of the foundation (v_2) for the rigid base (Figure 19) was produced by AA (approx. 37 mm), whereas the smallest was produced by ABL (approx. 1.4 mm). The largest uplift on the pebble layer was produced by AP and AA (approx. 14 mm). The largest permanent settlement on the left edge of the foundation of approximately 5 mm for the pebble layer was for AA (thick layer with large pebbles). The consequence of the different permanent vertical settlement of the left edge and right edge of

the foundation is the rotation of the model and the occurrence of an additional permanent horizontal displacement u_1.

8.3. Comparison of Experimental Results for Models MSB and MSSB.
Table 1 presents the maximum values of some of the measured experimental results for building models MSB and MSSB on a rigid base and on the pebble layer as well as the ratio of these values. Note that the efficiency of the pebble layer depends on the stiffness of the building model and the type of accelerogram (earthquake characteristics). The values in Table 1 are shown in Figures 20–23, which provide a better visual insight into the ratio of measured
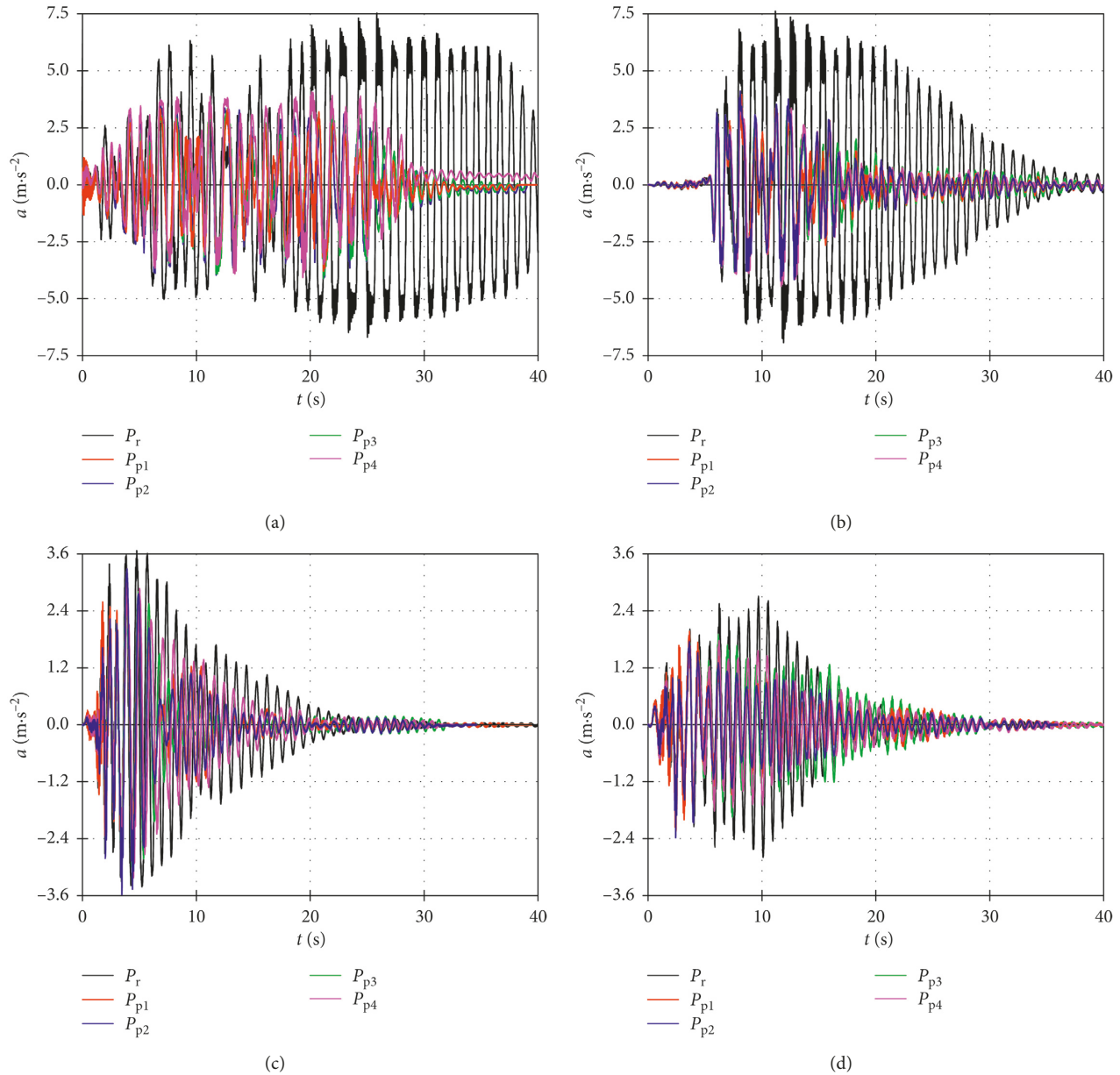
FIGURE 15: Horizontal acceleration of the mass center at the column top (a) for MSSB. (a) Artificial accelerogram (AA). (b) Accelerogram Petrovac (AP). (c) Accelerogram Ston (AS). (d) Accelerogram B. Luka (ABL).

maximum values on the rigid base and pebble layer, i.e., a better insight into the effectiveness of the pebble layer compared to the rigid base.

8.3.1. Artificial Accelerogram (AA). For the MSB model of the stiff building, compared to the rigid base case, the pebble layer reduced the horizontal displacement of the mass center at the column top by 70% and reduced the uplift of foundation by 77%. The horizontal acceleration of the mass center at the column top (inertial forces) was reduced by 50%, and the strains/stresses at the bottom of the steel column were reduced by 47%. There is remarkable similarity between the acceleration of the

mass at the column top and the strains at the bottom of the steel column because the strains are the dominant consequence of the inertial force of mass at the column top.

For the MSSB model of the medium-stiff building, compared to the rigid base case, the pebble layer reduced the horizontal displacement of the mass center at the column top by 38% and reduced the uplift of the foundation by 56%. The horizontal acceleration of the mass center at the column top (inertial forces) was reduced by 42%, and the strains/stresses at the bottom of the steel column were reduced by 47%.

The pebble layer efficiency from the aspect of strain reduction at the bottom of the steel column is similar for the
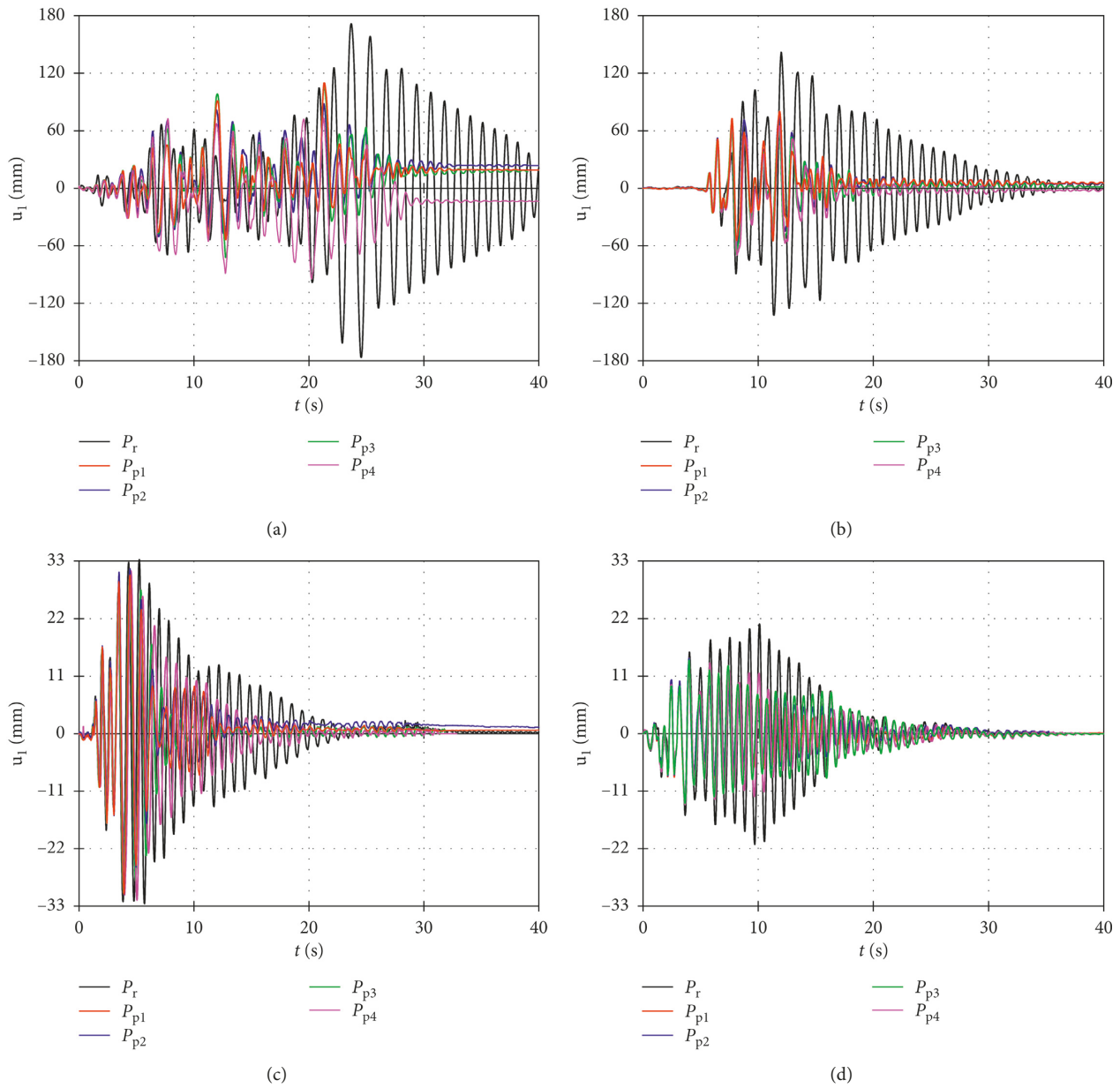
FIGURE 16: Horizontal displacement of the mass center at the column top (u_1) for MSSB. (a) Artificial accelerogram (AA). (b) Accelerogram Petrovac (AP). (c) Accelerogram Ston (AS). (d) Accelerogram B. Luka (ABL).

MSB and MSSB models, and from the aspect of displacement reduction, the MSB model is more favorable. The strains at the bottom of the steel column are several times higher for the MSSB model than for the MSB model. Large horizontal displacements of the mass center at the column top are the consequence of the adopted small dimensions of the foundation.

8.3.2. Accelerogram Petrovac (AP). For the MSB model of the stiff building, compared to the rigid base case, the pebble layer reduced the horizontal displacement of the mass center at the column top by 29%. The uplift of the foundation was reduced by 31%. The horizontal acceleration of the mass center at the column top and strain at the bottom of the steel column were reduced by 53%.

For the MSSB model of the medium-stiff building, compared to the rigid base case, the pebble layer reduced the horizontal displacement of the mass center at the column top by 44% and the uplift of the foundation by 52%. The horizontal acceleration of the mass center at the column top (inertial forces) was reduced by 41%, and the strains/stresses at the bottom of the steel column were reduced by 47%.

From the aspect of strain/stress reduction at the bottom of the steel column, the efficiency of the pebble layer is similar for the MSB and MSSB models. Moreover, the strain reduction at the bottom of the steel column is similar for AA and AP.
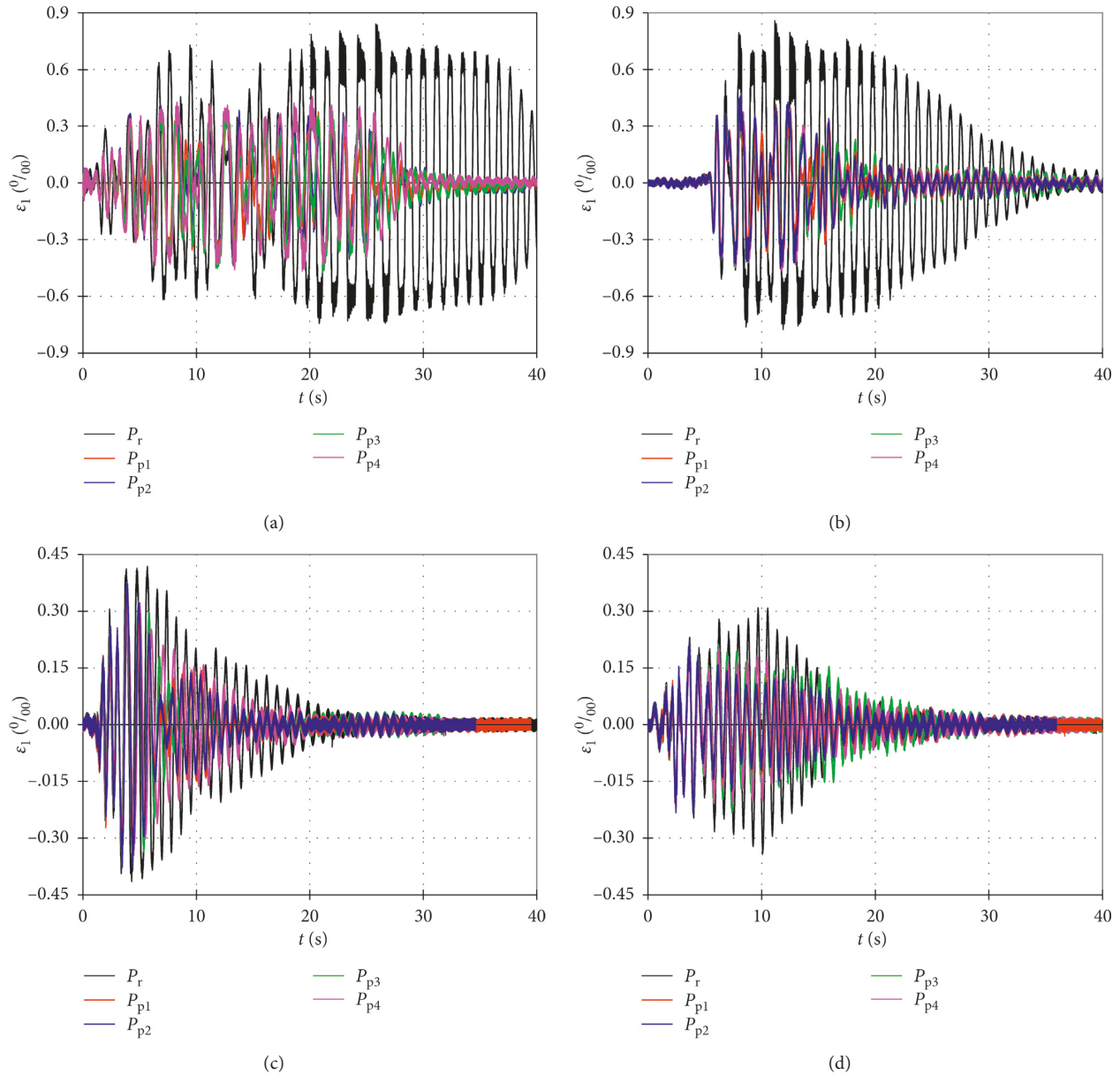
FIGURE 17: Vertical strain on the right bottom side of the steel column (ε_1) for MSSB. (a) Artificial accelerogram (AA). (b) Accelerogram Petrovac (AP). (c) Accelerogram Ston (AS). (d) Accelerogram B. Luka (ABL).

8.3.3. Accelerogram Ston (AS). Compared to AP and AA, AS produced several times smaller horizontal displacements of the mass center at the column top. However, regarding strains/stresses at the bottom of the steel column, no such difference was found. AS develops low values of displacement and stress/strain reduction because that excitation did not produce strong oscillations of the pebble layer. For the MSB model, compared to the rigid base case, the pebble layer reduced the strains at the bottom of the steel column by 26%. For the MSSB model, the reduction was only 8%. Obviously, the pebble layer for AS showed significantly lower efficiency than those for AA and AP and generated strains/stresses in models for AS that were significantly lower.

8.3.4. Accelerogram B. Luka (ABL). Generally, the comments in Section 8.3.3 regarding AS are valid. Compared to AS, the efficiency of the pebble layer in terms of strain reduction at the bottom of the steel column is higher for ABL. Compared to the rigid base case, the pebble layer reduced the strain at the bottom of the steel column by 28% and 31% on the MSB and MSSB model, respectively.

9. Conclusions

Based on the experimental research results of the behavior of two tested building models with fundamental periods $T = 0.05$ s (the so-called model of stiff building (MSB)) and $T = 0.6$ s (the so-called model of medium-stiff building (MSSB))
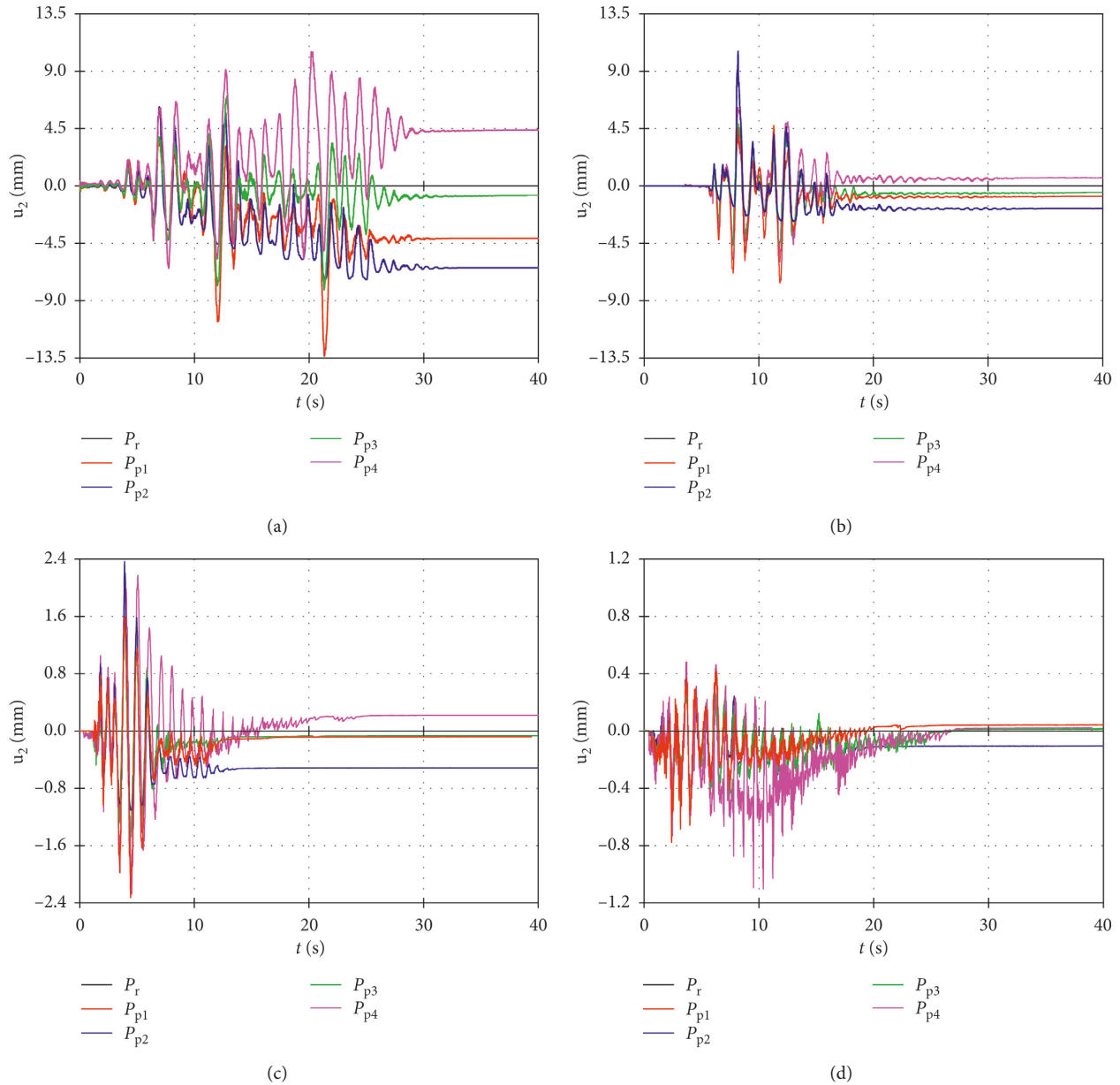
FIGURE 18: Horizontal displacement at the foundation top (u_2) for MSSB. (a) Artificial accelerogram (AA). (b) Accelerogram Petrovac (AP). (c) Accelerogram Ston (AS). (d) Accelerogram B. Luka (ABL).

supported on a rigid base and a pebble layer with a thicknesses of 0.3 m (the so-called thin layer) and 0.6 m (the so-called thick layer), with pebble fractions of 4–8 mm (the so-called small pebbles) and 16–32 mm (the so-called large pebbles), exposed to four different horizontal accelerograms (artificial accelerogram—AA, accelerogram Petrovac—AP, accelerogram Ston—AS, and accelerogram B. Luka—ABL) with model stresses in the elastic area, the following conclusions can be drawn:

   (i) In relation to the behavior of the building models with the foundation on a rigid base, the use of a natural stone pebble layer under the foundation resulted in a much more favorable response to seismic base accelerations.

   (ii) The strain/stress reduction in the column above the foundation for AA, AP, AS, and ABL was 47%, 53%, 26%, and 28% for the MSB model and 47%, 47%, 8%, and 31%, respectively, for the MSSB model. Note that all stresses were in the elastic area, without material nonlinearity of the structure.

   (iii) The reduction in the horizontal displacement of the mass center at the column top for AA, AP, AS, and ABL was 70%, 29%, 0%, and 46% for MSB and 38%, 44%, 5%, and 31%, respectively, for MSSB.

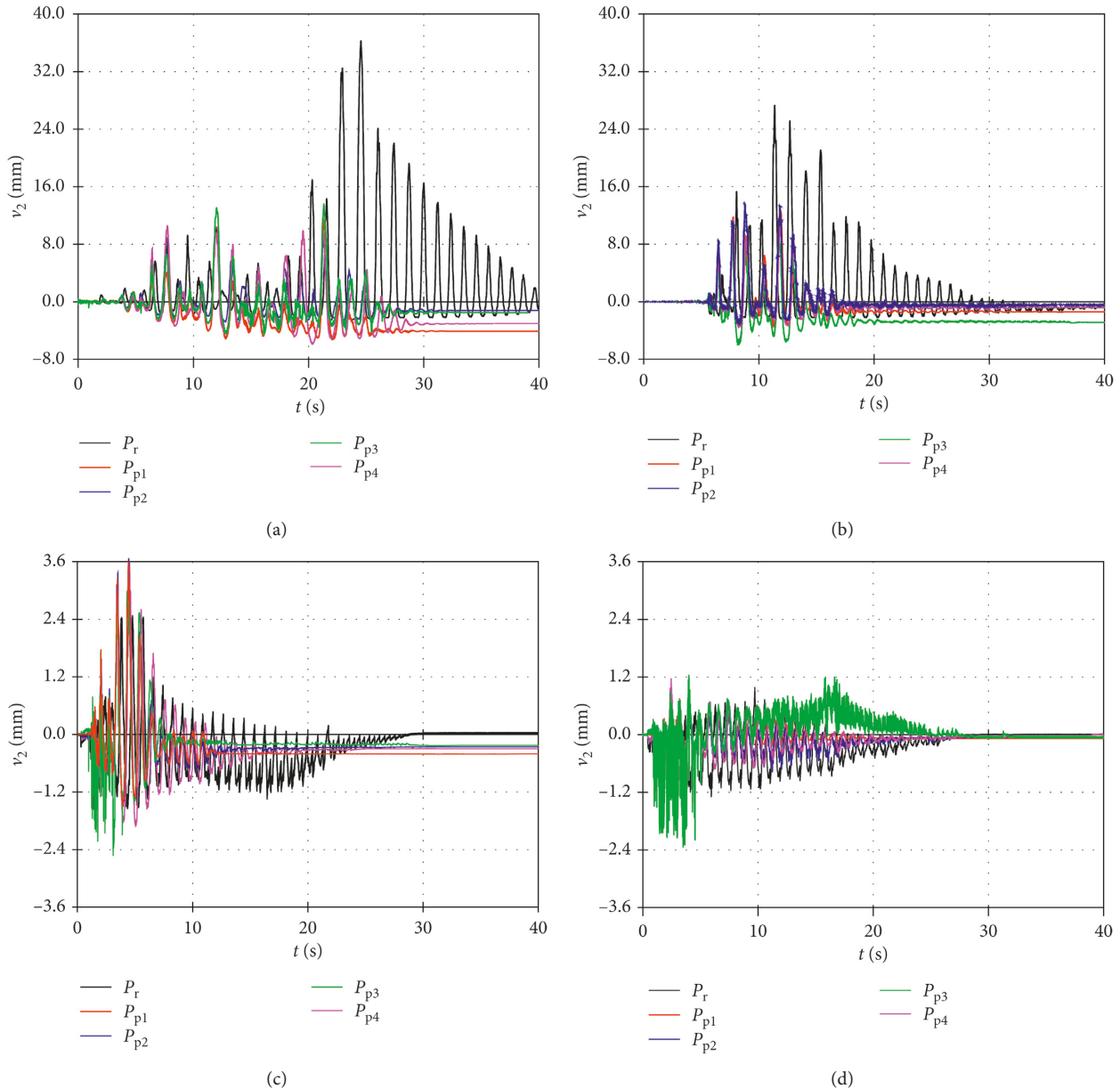   (iv) The efficiency of the pebble layer for MSSB was almost equal as that for MSB.

(a)

(b)

(c)

(d)

FIGURE 19: Foundation vertical displacement at the left edge (v_2) for MSSB. (a) Artificial accelerogram (AA). (b) Accelerogram Petrovac (AP). (c) Accelerogram Ston (AS). (d) Accelerogram B. Luka (ABL).

(v) The pebble layer efficiency in the performed tests was relatively independent of the thickness (0.3 m and 0.6 m) and the pebble fraction (4–8 mm and 16–32 mm).

(vi) According to the tests results, a small permanent horizontal displacement and vertical settlement (rotation) of the foundation on a real building on the considered pebble layer is expected.

(vii) Based on the results of the conducted experimental research, it can be expected that a stone pebble layer below the foundation of a real building is a sufficiently efficient low-technology seismic base isolation method, which is particularly useful

for low-cost buildings in less-developed countries. However, firm conclusions require further research.

(viii) Although the above conclusions are based on the results of tests on small-scale models, we believe that they are also applicable to buildings in practice. This is explained by the fact that small-scale models had a fundamental free oscillation period as full-scale buildings and that only relative effects of the considered parameters were tested on small-scale models.

(ix) It should be noted that the proposed concept of seismic base isolation would not be efficient in

TABLE 1: Maximum values of some measured experimental results and their ratios.

Applied excitation	Building model	Horizontal displacement of the block center			Vertical uplift of the foundation			Acceleration of the block center			Strain at the bottom of the column		
		u_1 (mm)	u_1^* (mm)	u_1^*/u_1	v_1, v_2 (mm)	v_1^*, v_2^* (mm)	$(v_1^*, v_2^*)/(v_1, v_2)$	a (m·s^{-2})	a^* (m·s^{-2})	a^*/a	$\varepsilon_1, \varepsilon_2$ (‰)	$\varepsilon_1^*, \varepsilon_2^*$ (‰)	$(\varepsilon_1^*, \varepsilon_2^*)/(\varepsilon_1, \varepsilon_2)$
Artificial	MSB	150	45	0.30	64	15	0.23	11.6	5.5	0.47	0.055	0.029	0.53
Accelerogram	MSSB	173	107	0.62	39	17	0.44	7.6	4.4	0.58	0.850	0.460	0.53
Accelerogram	MSB	120	85	0.71	51	35	0.69	12.1	5.7	0.47	0.058	0.027	0.47
Petrovac	MSSB	142	80	0.56	28	13.5	0.48	7.6	4.5	0.59	0.870	0.460	0.53
Accelerogram	MSB	16.2	16.5	1.02	6.8	5.5	0.81	6.5	5.2	0.80	0.031	0.023	0.74
Ston	MSSB	33.6	32	0.95	3.2	3.7	1.16	3.7	3.7	1.00	0.415	0.380	0.92
Accelerogram	MSB	12	6.5	0.54	4.4	1.7	0.39	5.8	4.1	0.71	0.025	0.018	0.72
B. Luka	MSSB	21	14.5	0.69	1.4	2.3	1.64	2.8	2.4	0.86	0.320	0.220	0.69

u_1, v_1, v_2, a, ε_1, and ε_2 are the maximum values for the rigid base. u_1^*, v_1^*, v_2^*, a^*, ε_1^*, and ε_2^* are the maximum values for the pebble layer.

(i) Horizontal displacement of the block center

(ii) Vertical uplift of the foundation

(iii) Acceleration of the block center

(iv) Strain at the bottom of the column

(a) Model of stiff building (MSB)

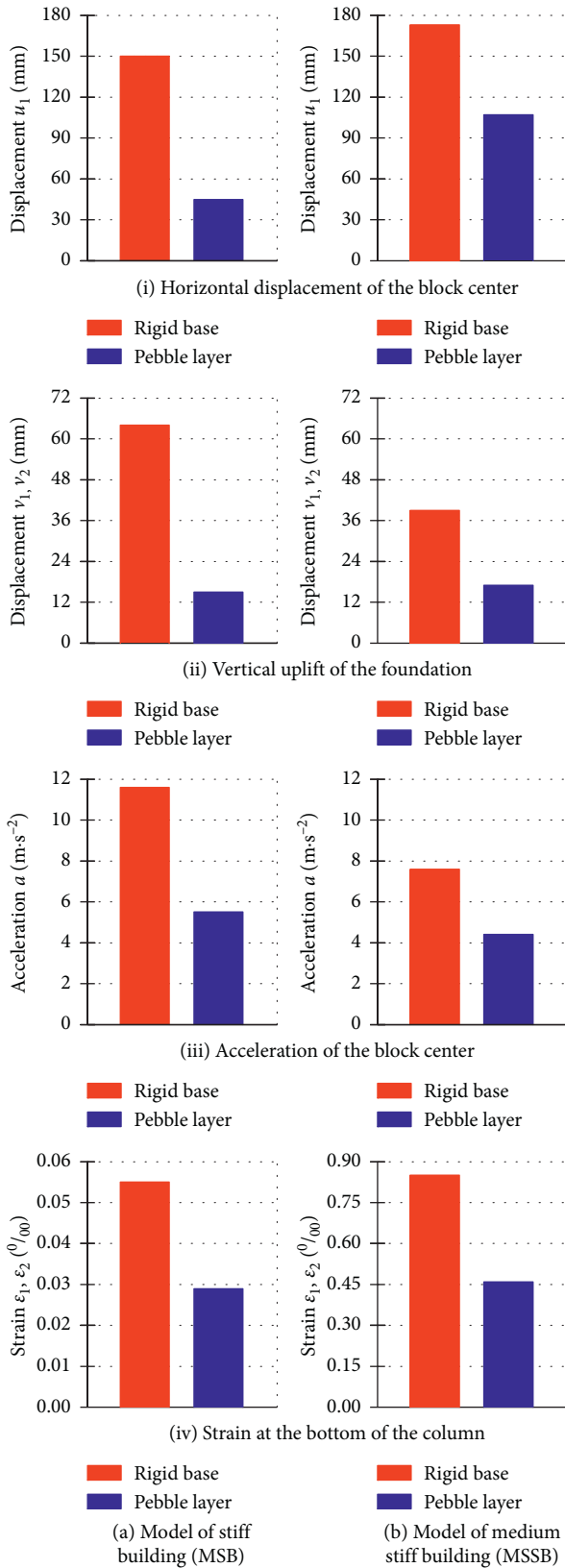(b) Model of medium stiff building (MSSB)

FIGURE 20: Some maximum measured values for an artificial accelerogram (AA). (a) Model of stiff building (MSB). (b) Model of medium stiff building (MSSB).
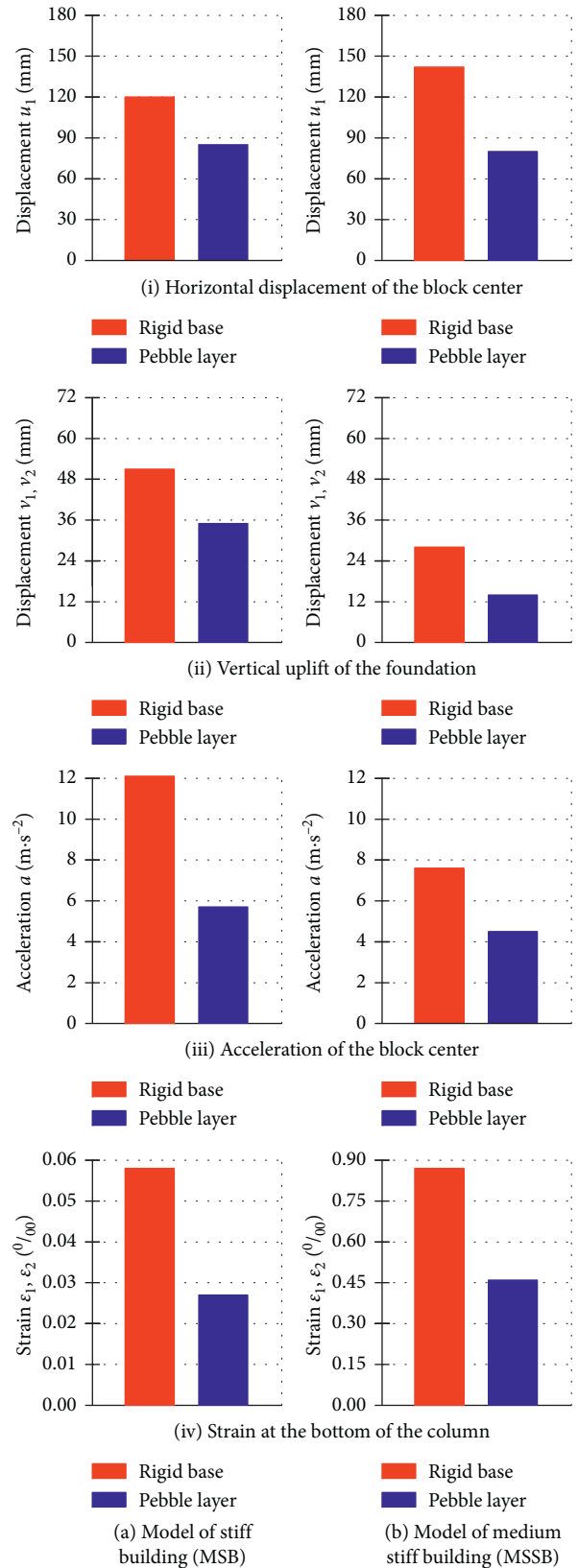
FIGURE 21: Some maximum measured values for the accelerogram Petrovac (AP). (a) Model of stiff building (MSB). (b) Model of medium stiff building (MSSB).
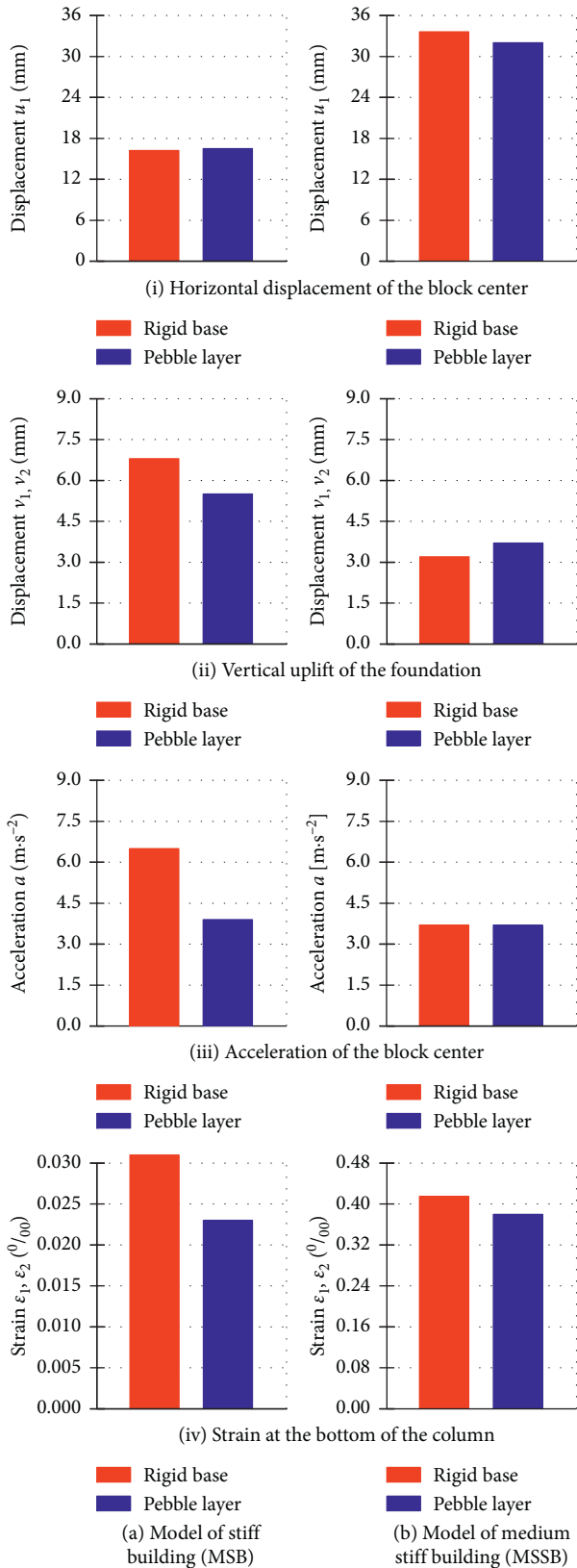
FIGURE 22: Some maximum measured values for the accelerogram Ston (AA). (a) Model of stiff building (MSB). (b) Model of medium stiff building (MSSB).
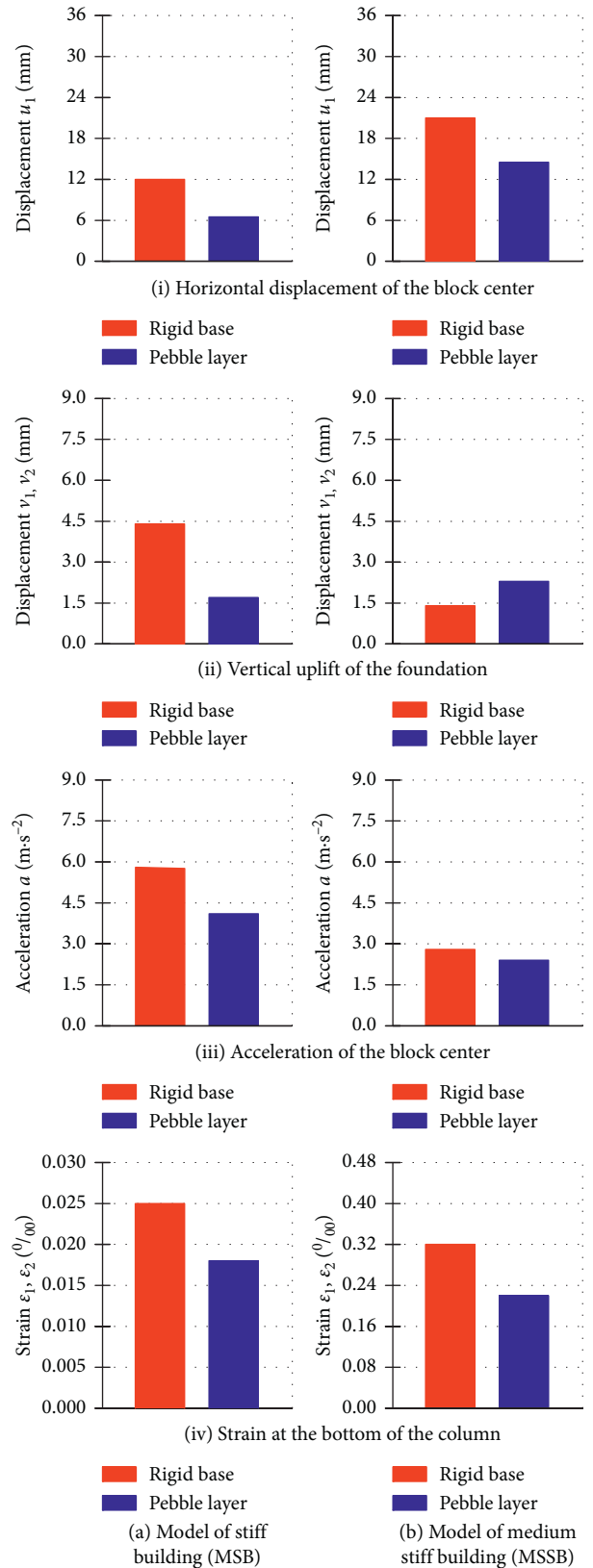

FIGURE 23: Some maximum measured values for the accelerogram B. Luka (ABL). (a) Model of stiff building (MSB). (b) Model of medium stiff building (MSSB).

earthquakes where the vertical acceleration component is dominant in relation to the horizontal component.

Data Availability

The data used to support the findings of this study are included within the article.
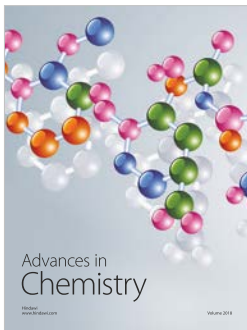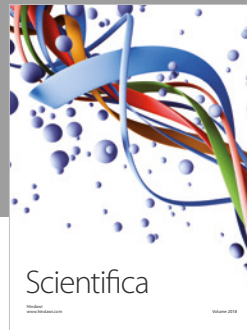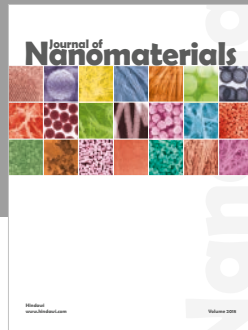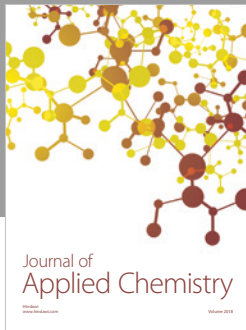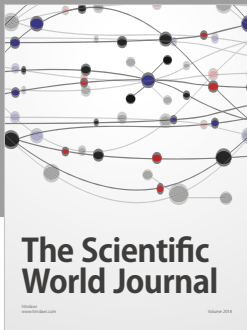
Conflicts of Interest

The authors declare that there are no conflicts of interest regarding the publication of this paper.

Acknowledgments

References

[1] I. Doudoumis, P. Papadopoulos, and T. Papaliangas, "Low-cost base isolation system on artificial soil layers with low shearing resistance," in *Proceedings of the 12th European Conference on Earthquake Engineering*, London, UK, September 2002.

[2] M. K. Yegian and U. Kadakkal, "Foundation isolation for seismic protection using a smooth synthetic liner," *Journal of Geotechnical and Geo-Environmental Engineering*, vol. 130, no. 11, pp. 1121–1130, 2004.

[3] M. K. Yegian and M. Catan, "Soil isolation for seismic protection using a smooth synthetic liner," *Journal of Geotechnical and Geo-Environmental Engineering*, vol. 130, no. 11, pp. 1131–1139, 2004.

[4] H. Xiao, J. W. Butterworth, and T. Larkin, "Low-technology techniques for seismic isolation," in *Proceedings of NZSEE Conference*, New Zealand, 2004.

[5] H. H. Tsang, "Seismic isolation by rubber–soil mixtures for developing countries," *Earthquake Engineering & Structural Dynamics*, vol. 37, no. 2, pp. 283–303, 2008.

[6] J. Radnić, N. Grgić, D. Matešan, and G. Baloević, "Shake table testing of reinforced concrete columns with different layout size of foundation," *Materialwissenschaft und Werkstofftechnik*, vol. 46, no. 4-5, pp. 348–367, 2015.

[7] I. Banović, J. Radnić, N. Grgić, and D. Matešan, "The use of limestone sand for the seismic base isolation of structures," *Advances in Civil Engineering*, vol. 2018, Article ID 9734283, 12 pages, 2018.

[8] W. Xiong and Y. Li, "Seismic isolation using granulated tire–soil mixtures for less-developed regions: experimental validation," *Earthquake Engineering & Structural Dynamics*, vol. 42, pp. 2187–2193, 2013.

[9] H. H. Tsang, S. H. Lo, X. Xu, and S. M. Neaz, "Seismic isolation for low-to-medium-rise buildings using granulated rubber–soil mixtures: numerical study," *Earthquake Engineering & Structural Dynamics*, vol. 41, no. 14, pp. 2009–2024, 2012.

[10] K. Pitilakis, S. Karapetrou, and K. Tsagdi, "Numerical investigation of the seismic response of RC buildings on soil replaced with rubber–sand mixtures," *Soil Dynamics & Earthquake Engineering*, vol. 79, pp. 237–252, 2015.

[11] A. Panjamani, M. D. Ramegowda, and R. Divyesh, "Low cost damping scheme for low to medium rise buildings using rubber soil mixtures," *Japanese Geotechnical Society Special Publication*, vol. 3, no. 2, pp. 24–28, 2015.

[12] S. Bandyopadhyay, A. Sengupta, and G. R. Reddy, "Performance of sand and shredded rubber tire mixture as a natural base isolator for earthquake protection," *Earthquake Engineering & Engineering Vibration*, vol. 14, no. 4, pp. 683–693, 2015.

[13] S. J. Patil, G. R. Reddy, R. Shivshankar, R. Babu, B. R. Jayalekshmi, and B. Kumar, "Seismic base isolation for structures using river sand," *Earthquakes and Structures*, vol. 10, no. 4, pp. 829–847, 2016.

[14] R. P. Nanda, P. Agarwal, and M. Shrikhande, "Frictional base isolation by geotextiles for brick masonry buildings," *Geosynthetics International*, vol. 17, no. 1, pp. 48–55, 2010.

[15] R. P. Nanda, P. Agarwal, and M. Shrikhande, "Base isolation by geosynthetic for brick masonry buildings," *Journal of Vibration and Control*, vol. 18, no. 6, pp. 903–910, 2012.

[16] R. P. Nanda, M. Shrikhande, and P. Agarwal, "Effect of ground motion characteristics on the pure friction isolation system," *Earthquakes and Structures*, vol. 3, no. 2, pp. 169–180, 2012.

[17] R. P. Nanda, M. Shrikhande, and P. Agarwal, "Low-cost base-isolation system for seismic protection of rural buildings," *Practice Periodical on Structural Design and Construction*, vol. 21, no. 1, 2015.

[18] M. Qamaruddin and S. Ahmad, "Seismic response of pure-friction base isolation masonry building with restricted base sliding," *Journal of Engineering Research*, vol. 4, no. 1, pp. 82–94, 2007.

[19] S. Ahmad, F. Ghani, and R. Adil, "Seismic friction base isolation performance using demolished waste in masonry housing," *Construction and Building Materials*, vol. 23, no. 1, pp. 146–152, 2009.

[20] EN 1998-1:2004, *Eurocode 8: Design of Structures for Earthquake Resistance. Part 1: General Rules, Seismic Actions and Rules for Buildings*, European Committee for Standardization, Brussels, Belgium, 2004.

[21] N. Ambraseys, P. Smit, R. Sigbjörnsson, P. Suhadolc, and M. Margaris, *Internet-Site for European Strong-Motion Data, EVR1-CT-1999-40008*, European Commission, Directorate-General XII, Environmental and Climate Programme, Brussels, Belgium, 2001, http://www.isesd.hi.is/ESD_Local/frameset.htm.

The Scientific
World Journal

Journal of
Applied Chemistry

Journal of
Nanomaterials

Scientifica

International Journal of
Polymer Science

Advances in
Chemistry

Advances in
Physical Chemistry

International Journal of
Analytical Chemistry

Hindawi

Submit your manuscripts at
www.hindawi.com

Advances in
Condensed Matter Physics

Journal of
Chemistry

International Journal of
Biomaterials

Advances in
High Energy Physics

Journal of
Engineering

Journal of
Nanotechnology

International Journal of
Corrosion

Journal of
Materials

BioMed
Research International

Advances in
Tribology

Advances in
Materials Science and Engineering